16th World Conference on Earthquake Engineering, 16WCEE 2017

Santiago Chile, January 9th to 13th 2017

Paper N° 1121

Registration Code: S-D1463144549

AN EXPLICIT QUADRATIC ALPHA NUMERICAL INTEGRATION ALGORITHM FOR FORCE-BASED HYBRID SIMULATION

B. Forouzan[1], N. Nakata[2]

[1] *Graduate student, Dept. of Civil and Envr. Engineering, Clarkson University, Potsdam, United State, forouzb@clarkson.edu*
[2] *Associate professor, Dept. of Civil and Envr. Engineering, Clarkson University, Potsdam, United State, nnakata@clarkson.edu*

Abstract

Hybrid simulation is a combination of physical testing and numerical simulation, which provides a powerful technique for dynamic testing of large and complex structural systems. While the hybrid simulation has been used in various applications, it has some limitations. One of the limitations is that force equilibrium is not always guaranteed because the conventional hybrid simulation is displacement based; the formulation is based on the displacement, which ensures only displacement compatibilities of unless an iterative approach is used. In some cases, displacement-based approach is not suitable and even applicable (e.g., testing of rigid specimen). This study presents an explicit numerical integration algorithm for force-based hybrid simulation. In the force-based hybrid simulation, the formulation/governing equation is calculated in terms of force first. The calculated force is then applied to the test specimen through a force control technique and the corresponding displacement is measured. The measured displacement is sent back to the numerical algorithm and the responses at the next step are updated based on the measured displacement and the responses at the previous steps. This paper presents a new force-based explicit numerical integration algorithm, so-called quadratic-alpha method. The proposed method is based on the quadratic interpolation of the equation of motion and consists of pre-experimental, experimental, and post-experimental processes to enable hybrid simulation. Formulation and background theories of the quadratic alpha method as well as the implementation flowchart are presented in the paper. Then, dynamic characteristics and stability of the method are discussed using discrete transfer functions. The stability assessment shows that the quadratic alpha method provides stable simulation for systems with different natural frequencies. The numerical simulation of the quadratic alpha method is performed for earthquake, wind and coastal storm surge loads with three restoring force models. While some discrepancies are found between the quadratic alpha method and the reference nonlinear dynamic analysis for highly nonlinear hysteresis models, the method is proven to be stable and provide reasonable accuracy for all of the considered scenarios.

Keywords: hybrid simulation; force-based formulation; explicit numerical method; force control.

1. Introduction

High performance simulation is essential in the area of natural hazards engineering for better understanding of phenomenon, assessment of design codes, and development of mitigation measures. One of the critical aspects in such simulation is fidelity of modeling. While computational approaches offer effective tools for modeling of loading, components, and systems, etc., there are still features that are difficult to model computationally. Those include nonlinearities, uncertainties, and unpredictabilities of structural members and subassemblies that are subject to complex and extreme loads. For simulation with such components, experimental modeling fulfills a crucial role and can be incorporated to ensure the fidelity of the simulation.

A technique that combines computational and experimental models is called hybrid simulation (a.k.a., hardware-in-the-loop, substructuring, etc.) [1]. Hybrid simulation is an efficient and cost-effective approach particularly when the computational models are not sufficient and the physical modeling of the entire system is not feasible. It has been extensively studied in the earthquake engineering field, ranging from development of techniques (e.g., real-time hybrid simulation) to its applications for performance assessment of structures [2-3]. However, hybrid simulation has not been methodically expanded to simulations of other hazards such as wind and tsunami.

To expand the hybrid simulation as a sound methodology to the other hazards, careful attentions have to be paid because of the limitations in the conventional hybrid simulation method. Two of the major limitations towards expansion are following: i) Loading in wind and tsunami is dependent on the geometric shape of the structure. Therefore, the loading has to be determined based on the structural geometry including deformation. However, the conventional hybrid simulation imposes prescribed displacement that controls the restoring force and the loading path within the structure whereas in reality the external load causes structural deformation that reaches force equilibrium. ii) Force equilibrium in the governing equations is not always satisfied at each time step, leaving unbalanced force. In earthquake simulation, this issue is tolerable because loading (e.g., input ground acceleration) is predefined and does not influence the stability of the simulation. However, in case of wind and tsunami simulations where deformation and loading are coupled, the unbalanced force exerts influence on the stability that becomes dependent on the loading. Both of the limitations are because the governing equations are solved in terms of displacement without iterative approaches in the conventional hybrid simulation.

A logical approach to overcome the above challenges is to solve the governing equations based on the force and to impose the prescribed force to determine the structural deformation as the results. We name such approach as force-based hybrid simulation. The concept of the force-based hybrid simulation may sound similar to the effective force testing (EFT). But, it should be clarified that they are different in essence because force-based hybrid simulation can accommodate deformation-dependent load by numerically solving the governing equations whereas the EFT cannot. For more details about the EFT, refer to Dimig et al [4] and Nakata [5].

This study presents a numerical integration method that enables force-based hybrid simulation for the assessment of structural performance under various hazards. The proposed method is named the quadratic alpha method in this paper and is based on the quadratic interpolation of the equations of motion in the formulation. Because it is an explicit method, it is suited for the implementation in hybrid simulation. This paper presents the detailed formulation and thorough investigation of the proposed method. The investigation includes theoretical assessment of the method in terms of stability and feasibility and numerical validation with linear and nonlinear structural models for earthquake, wind and coastal surge. The work presented here will serve as the preliminary groundwork for the design and implementation of the force-based hybrid simulation that is currently underway.

2. Formulation and algorithm of the quadratic alpha method

This study presents a new formulation of equations of motion for force-based hybrid simulation. The proposed formulation provides non-iterative solution algorithm and seamless integration of force control experiment into hybrid simulation, satisfying strict force equilibrium at each time step. The details of the formulation and algorithm of the force-based hybrid simulation are presented in this section.

2.1 Assumptions, requirements and problem statement

Dynamic responses of structures can be expressed in second-order differential equations known as the equations of motion shown below.

$$\mathbf{M}\ddot{\mathbf{x}}_n + \mathbf{C}\dot{\mathbf{x}}_n + \mathbf{r}_n = \mathbf{p}_n \tag{1}$$

where $\mathbf{M}$ and $\mathbf{C}$ are the mass matrix and damping matrix, respectively; $\ddot{\mathbf{x}}$, $\dot{\mathbf{x}}$, $\mathbf{x}$, $\mathbf{r}$ and $\mathbf{p}$ are the acceleration, velocity, displacement, restoring force and input force vector, respectively; and n is the step number.

Assuming that the input and responses up to the current step, $\mathbf{p}_i, \mathbf{x}_i, \dot{\mathbf{x}}_i, \ddot{\mathbf{x}}_i, \mathbf{r}_i \left(i = 1, \cdots, n\right)$, are given and that they satisfy Eq. (1), numerical integration algorithms have to solve the responses at the next step $n+1$ from $\mathbf{p}_{n+1}$. The algorithms for the force-based hybrid simulation need to meet further requirements and constraints such as following: i) force-based solution procedure: to incorporate the force-based hybrid simulation, the algorithms have to solve the governing equations based on the force, specifying the reference force at each step; ii) unbalanced force free algorithm: considering applications to wind and coastal hazard simulations, the algorithms have to strictly meet the force equilibrium at each step; and iii) no iterative approach: a deterministic procedure within each step is required to ensure steady procession in hybrid simulation.

The algorithm for the force-based hybrid simulation that is developed and investigated in this study, here referred to as force-based quadratic alpha-method, meets all of the above requirements and enables seamless integration of force control into hybrid simulation.

2.2 Force-based quadratic alpha-method

Given the previous and current responses up to step n that satisfy the equations of motion, the proposed quadratic alpha-method evaluates an equilibrium at an interpolated point between steps $n-1$ and n. The equations of motion at the interpolated point take the following form:

$$\mathbf{M}\bar{\ddot{\mathbf{x}}}_n + \mathbf{C}\bar{\dot{\mathbf{x}}}_n + \bar{\mathbf{r}}_n = \bar{\mathbf{p}}_n \tag{2}$$

where $\bar{\ddot{\mathbf{x}}}$, $\bar{\dot{\mathbf{x}}}$, $\bar{\mathbf{r}}$ and $\bar{\mathbf{p}}$ are the interpolated acceleration, velocity, restoring force and input force vectors, which are expressed as:

$$\bar{\ddot{\mathbf{x}}}_n = \alpha\ddot{\mathbf{x}}_{n-1} + \left(1-\alpha\right)\ddot{\mathbf{x}}_n \tag{3}$$

$$\bar{\dot{\mathbf{x}}}_n = \alpha\dot{\mathbf{x}}_{n-1} + \left(1-\alpha\right)\dot{\mathbf{x}}_n \tag{4}$$

$$\bar{\mathbf{r}}_n = \frac{1}{2}\alpha\left(1+\alpha\right)\mathbf{r}_{n-1} + \left(1-\alpha^2\right)\mathbf{r}_n - \frac{1}{2}\alpha\left(1-\alpha\right)\tilde{\mathbf{r}}_{n+1} \tag{5}$$

$$\bar{\mathbf{p}}_n = \frac{1}{2}\alpha\left(1+\alpha\right)\mathbf{p}_{n-1} + \left(1-\alpha^2\right)\mathbf{p}_n - \frac{1}{2}\alpha\left(1-\alpha\right)\mathbf{p}_{n+1} \tag{6}$$

where $\tilde{\mathbf{r}}_{n+1}$ is the extrapolated force at step $n+1$; and α is the interpolation parameter with the range of $0<\alpha<1$.

The interpolated acceleration and velocity terms are from linear spline between steps $n-1$ and n whereas the restoring force and input force terms are based on quadratic spline with steps $n-1$, n, and $n+1$. Note that while the spline forms are different, the interpolated axes in terms of step (i.e., equivalent time) are the same in all of the terms regardless of the selection of α. Eq. (2) still meets Eq. (1) at step n and $n-1$ at $\alpha=0$ and $\alpha=1$, respectively.

Because of the quadratic spline with step $n+1$ in the restoring force term, the equatios of motion in Eq. (2) can be solved in terms of the extrapolated restoring force. By substituting Eq. (5) into Eq. (2), the extrapolated force at step $n+1$ is expressed as:

$$\tilde{\mathbf{r}}_{n+1} = \frac{2}{\alpha(1-\alpha)}\left(\mathbf{M}\bar{\ddot{\mathbf{x}}}_n + \mathbf{C}\bar{\dot{\mathbf{x}}}_n - \tilde{\mathbf{p}}_n\right) \tag{7}$$

where

$$\tilde{\mathbf{p}}_n = \bar{\mathbf{p}}_n - \frac{1}{2}\alpha(1+\alpha)\mathbf{r}_{n-1} - \left(1-\alpha^2\right)\mathbf{r}_n \tag{8}$$

This extrapolated restoring force $\tilde{\mathbf{r}}_{n+1}$ is used as the reference force in the force-based hybrid simulation and imposed in experimental and numerical substructures to evaluate the force-displacement relationships. To reduce the impact of control errors in the experiment, the following correction step is suggested to incorporate in the experimental process.

$$\tilde{\mathbf{x}}_{n+1} = \left(\tilde{\mathbf{r}}_{n+1} - \tilde{\mathbf{r}}^m_{n+1}\right)\mathbf{K}^{-1} + \tilde{\mathbf{x}}^m_{n+1} \tag{9}$$

where $\tilde{\mathbf{r}}^m_{n+1}$ and $\tilde{\mathbf{x}}^m_{n+1}$ are the measured force and displacement, respectively; and $\mathbf{K}$ is the estimated tangent stiffness of the experimental substructure. The corrected experimental displacement $\tilde{\mathbf{x}}_{n+1}$ is then sent to the subsequent computational process to acquire the responses at step $n+1$.

2.3 Kinematic relations and unbalanced force correction procedure

The discrete integral forms in the Newmark method gives the kinematic relations of displacement and velocity with respect to acceleration as:

$$\tilde{\mathbf{x}}_{n+1} = \mathbf{x}_n + \Delta t\dot{\mathbf{x}}_n + \left(\frac{1}{2}-\beta\right)\Delta t^2\ddot{\mathbf{x}}_n + \beta\Delta t^2\tilde{\ddot{\mathbf{x}}}_{n+1} \tag{10}$$

$$\tilde{\dot{\mathbf{x}}}_{n+1} = \dot{\mathbf{x}}_n + (1-\gamma)\Delta t\ddot{\mathbf{x}}_n + \gamma\Delta t\tilde{\ddot{\mathbf{x}}}_{n+1} \tag{11}$$

By arranging these equations, the acceleration and velocity that are compatible with $\tilde{\mathbf{x}}_{n+1}$ are expressed as follows:

$$\tilde{\ddot{\mathbf{x}}}_{n+1} = \left(1-\frac{1}{2\beta}\right)\ddot{\mathbf{x}}_n - \frac{\dot{\mathbf{x}}_n}{\beta\Delta t} + \frac{\tilde{\mathbf{x}}_{n+1}-\mathbf{x}_n}{\beta\Delta t^2} \tag{12}$$

$$\tilde{\dot{\mathbf{x}}}_{n+1} = \dot{\mathbf{x}}_n + (1-\gamma)\Delta t\ddot{\mathbf{x}}_n + \gamma\Delta t\left\{\frac{1}{\beta\Delta t^2}\left(\tilde{\mathbf{x}}_{n+1} - \mathbf{x}_n - \Delta t\dot{\mathbf{x}}_n\right) - \left(\frac{1}{2\beta}-1\right)\ddot{\mathbf{x}}_n\right\} \tag{13}$$

The responses at this prediction step may not satisfy the equilibrium equation in (1), which leads to an unbalanced force that is defined as:

$$\mathbf{e}_{n+1} = -\mathbf{M}\tilde{\ddot{\mathbf{x}}}_{n+1} - \mathbf{C}\tilde{\dot{\mathbf{x}}}_{n+1} - \tilde{\mathbf{r}}_{n+1} + \mathbf{p}_{n+1} \tag{14}$$

By taking the difference with the equations of motion at step $n+1$ that strictly satisfy the equilibrium conditions, the above unbalanced force can be expressed in terms of acceleration, velocity and restoring force differences.

$$\mathbf{e}_{n+1} = \mathbf{M}\left(\ddot{\mathbf{x}}_{n+1} - \tilde{\ddot{\mathbf{x}}}_{n+1}\right) + \mathbf{C}\left(\dot{\mathbf{x}}_{n+1} - \tilde{\dot{\mathbf{x}}}_{n+1}\right) + \left(\mathbf{r}_{n+1} - \tilde{\mathbf{r}}_{n+1}\right) \tag{15}$$

Each of the above response difference can be expressed as:

$$\ddot{\mathbf{x}}_{n+1} - \tilde{\ddot{\mathbf{x}}}_{n+1} = \frac{1}{\beta \Delta t^2}\Delta\mathbf{x}_{n+1} \tag{16}$$

$$\dot{\mathbf{x}}_{n+1} - \tilde{\dot{\mathbf{x}}}_{n+1} = \frac{\gamma}{\beta \Delta t}\Delta\mathbf{x}_{n+1} \tag{17}$$

$$\mathbf{r}_{n+1} - \tilde{\mathbf{r}}_{n+1} = \mathbf{K}\Delta\mathbf{x}_{n+1} \tag{18}$$

where $\Delta\mathbf{x}_{n+1}\left(= \mathbf{x}_{n+1} - \tilde{\mathbf{x}}_{n+1}\right)$ is the displacement difference that is required to eliminate the unbalanced force at step $n+1$. By substituting equations (16-18) into (15), the displacement difference can be solved as:

$$\Delta\mathbf{x}_{n+1} = \left(\frac{\mathbf{M}}{\beta\Delta t^2} + \frac{\mathbf{C}\gamma}{\beta\Delta t} + \mathbf{K}\right)^{-1}\mathbf{e}_{n+1} \tag{19}$$

By substituting the displacement difference into the Eqs. (16)-(18), the converged response at step $n+1$ are obtained. These responses will strictly satisfy the equilibrium conditions at step $n+1$, incorporating force-displacement relations from force-controlled experiment. This process completes the entire procedure of a single step in the proposed quadratic alpha method. The process will be repeated.

2.4 Implementation diagram

To facilitate the implementation of the quadratic alpha method, the essential processes are shown in Fig.1. Besides the initialization, a single simulation step in the quadratic alpha method consists of three phases: namely pre-experimental computation (a.k.a., the predictor); experimental process; and post-experimental computation (a.k.a., the corrector). The pre-experimental computation includes steps 2 and 3 to specify the reference force that is to be imposed in the experiment. The experimental phase, step 4, is the loading on the structure using force-controlled technique. The post-experimental phase includes steps 5 to 9 to solve for the convergence parameter and update the responses at the next step.

3. Stability and Application Feasibility Assessment

Stability and accuracy are the two most important characteristics in the numerical integration algorithms. While accuracy can vary depending on the simulation conditions (i.e., model, input, nonlinearity, etc.), stability can be theoretically and systematically assessed with linearization. Prior to the numerical simulations in the next section that discusses accuracy, this section presents stability assessment of the quadratic alpha method using discrete transfer functions. Furthermore, sensitivity of the simulation parameters is also evaluated herein.

3.1 Discrete Transfer Functions

For linearized models, discrete transfer functions of the responses in the quadratic alpha method can be derived by taking the Z transform of the equations in the previous section. Table 1 list the transfer functions from the input force to the converged displacement $\mathbf{x}$ and the converged force $\mathbf{r}$ for a single degree of freedom linear model. In the transfer functions, following new parameters are introduced: m as the mass, ξ as the damping ratio, ω_n as the angular natural frequency, K_{EXP} as the true stiffness of the experimental system; K_{EST} as the estimated stiffness in the algorithm; $\mu(=K_{EST}/K_{EXP})$ as the ratio between K_{EST} and K_{EXP}; and $\lambda(=\omega_n\Delta t)$ as the frequency ratio.

Initialization

Step 1. Set parameters $\mathbf{M},\mathbf{C},\mathbf{K},\alpha,\beta,\gamma$ and Δt and initial conditions $\dot{\mathbf{x}}_n,\ddot{\mathbf{x}}_n,\mathbf{r}_n\,(n=0 \text{ and } 1)$

Pre-experimental computation

Step 2. Calculate the interpolated terms

$$\ddot{\bar{\mathbf{x}}}_n=\alpha\ddot{\mathbf{x}}_{n-1}+(1-\alpha)\ddot{\mathbf{x}}_n \qquad \dot{\bar{\mathbf{x}}}_n=\alpha\dot{\mathbf{x}}_{n-1}+(1-\alpha)\dot{\mathbf{x}}_n$$

$$\bar{\mathbf{p}}_n=\frac{1}{2}\alpha(1+\alpha)\mathbf{p}_{n-1}+(1-\alpha^2)\mathbf{p}_n-\frac{1}{2}\alpha(1-\alpha)\mathbf{p}_{n+1} \qquad \hat{\mathbf{p}}_n=\bar{\mathbf{p}}_n-\frac{1}{2}\alpha(1+\alpha)\mathbf{r}_{n-1}-(1-\alpha^2)\mathbf{r}_n$$

Step 3. Calculate the reference force $\tilde{\mathbf{r}}_{n+1}=\dfrac{2}{\alpha(1-\alpha)}\left(\mathbf{M}\ddot{\bar{\mathbf{x}}}_n+\mathbf{C}\dot{\bar{\mathbf{x}}}_n-\hat{\mathbf{p}}_n\right)$

Experimental process

Step 4. Experimental process: Impose $\tilde{\mathbf{r}}_{n+1}$ and measure $\tilde{\mathbf{r}}^m_{n+1}$ and $\tilde{\mathbf{x}}^m_{n+1}$

Post experimental computation

Step 5. Correct the effect of control error $\tilde{\mathbf{x}}_{n+1}=\left(\tilde{\mathbf{r}}_{n+1}-\tilde{\mathbf{r}}^m_{n+1}\right)\mathbf{K}^{-1}+\tilde{\mathbf{x}}^m_{n+1}$

Step 6. Obtain acceleration and velocity that correspond to $\tilde{\mathbf{x}}_{n+1}$

$$\ddot{\tilde{\mathbf{x}}}_{n+1}=\left(1-\frac{1}{2\beta}\right)\ddot{\mathbf{x}}_n-\frac{\dot{\mathbf{x}}_n}{\beta\Delta t}+\frac{\tilde{\mathbf{x}}_{n+1}-\mathbf{x}_n}{\beta\Delta t^2} \qquad \dot{\tilde{\mathbf{x}}}_{n+1}=\dot{\mathbf{x}}_n+(1-\gamma)\Delta t\ddot{\mathbf{x}}_n+\gamma\Delta t\ddot{\tilde{\mathbf{x}}}_{n+1}$$

Step 7. Compute the unbalanced force $\mathbf{e}_{n+1}=-\mathbf{M}\ddot{\tilde{\mathbf{x}}}_{n+1}-\mathbf{C}\dot{\tilde{\mathbf{x}}}_{n+1}-\tilde{\mathbf{r}}_{n+1}+\mathbf{p}_{n+1}$

Step 8. Calculate the incremental displacement $\Delta\mathbf{x}_{n+1}=\left(\dfrac{\mathbf{M}}{\beta\Delta t^2}+\dfrac{\mathbf{C}\gamma}{\beta\Delta t}+\mathbf{K}\right)^{-1}\mathbf{e}_{n+1}$

Step 9. Update the responses at step *n+1*

$$\mathbf{x}_{n+1}=\tilde{\mathbf{x}}_{n+1}+\Delta\mathbf{x}_{n+1} \qquad \dot{\mathbf{x}}_{n+1}=\dot{\tilde{\mathbf{x}}}_{n+1}+\frac{\gamma}{\beta\Delta t}\Delta\mathbf{x}_{n+1}$$

$$\ddot{\mathbf{x}}_{n+1}=\ddot{\tilde{\mathbf{x}}}_{n+1}+\frac{1}{\beta\Delta t^2}\Delta\mathbf{x}_{n+1} \qquad \mathbf{r}_{n+1}=\tilde{\mathbf{r}}_{n+1}+\mathbf{K}\Delta\mathbf{x}_{n+1}$$

Go back to step 2 with an increment of the step number

Fig.1 – Essential processes in the NF numerical integration algorithm for force-based hybrid simulation.

It can be observed that the denominators of the both transfer functions are identical fourth-order polynomial of the function z. This denominator polynomial is the characteristic equation of the quadratic alpha algorithm. The stability of the system can be evaluated by the roots of this characteristic equation. On the other hand, the forms and even the orders of the numerator are different; the displacement transfer function has the third order numerator while the force transfer function has the fourth order numerator. This fact implies that the displacement and force in the quadratic alpha method have different characteristics and accuracy. It is also worth mentioning that the transfer functions are not dependent on the interpolation parameter α.

3.2 Frequency responses and application assessment

The discrete transfer functions obtained above provide frequency responses of the systems with the quadratic alpha method. Based on the characteristics in the frequency responses, application feasibility of the quadratic alpha method is assessed herein.

Fig.2 shows frequency responses of three different systems with the quadratic alpha method. The difference is in the natural frequency f_n of each system; Figure (a), (b), and (c) are for f_n at 1.0, 10.0 and 25.0 (Hz), respectively. The other parameters here are $m=1$ (kg), $\xi=0.05$, $\beta=0.5$, $\gamma=0.5$, $dt=0.01$ (sec), and $\mu=1$ in all of the cases.

Table 1. Discrete transfer function from the input force to the converted displacement and force.

$H(z)=c\dfrac{b_1+b_2z^{-1}+b_3z^{-2}+b_4z^{-3}+b_5z^{-4}}{a_1+a_2z^{-1}+a_3z^{-2}+a_4z^{-3}+a_5z^{-4}}$			
		H_x	H_r
		$c=1/K_{\exp}$	$c=1$
i	a_i	b_i	b_i
1	$1+2\gamma\xi\lambda+\beta\mu\lambda^2$	$\beta\mu$	$1-\mu-2\gamma\xi(\mu-1)\lambda+\beta\mu\lambda^2$
2	$2\mu-4+2\xi(2\gamma\mu-4\gamma+1)\lambda+\mu\left(\gamma-2\beta+\frac{1}{2}\right)\lambda^2$	$\mu\left(\gamma-2\beta+\frac{1}{2}\right)$	$4\mu-4+2\xi(4\gamma-1)(\mu-1)\lambda+\mu\left(\gamma-2\beta+\frac{1}{2}\right)\lambda^2$
3	$6-5\mu+2\xi(6\gamma+2\mu-5\gamma\mu-3)\lambda+\mu\left(\beta-\gamma+\frac{1}{2}\right)\lambda^2$	$\mu\left(\beta-\gamma+\frac{1}{2}\right)$	$6-6\mu-6\xi(2\gamma-1)(\mu-1)\lambda+\mu\left(\beta-\gamma+\frac{1}{2}\right)\lambda^2$
4	$4\mu-4+2\xi(4\gamma-3)(\mu-1)\lambda$	0	$4\mu-4+2\xi(4\gamma-3)(\mu-1)\lambda$
5	$1-\mu-2\xi(\gamma-1)(\mu-1)\lambda$	0	$1-\mu-2\xi(\gamma-1)(\mu-1)\lambda$

First and foremost, the quadratic alpha method is stable in all of the three cases if the estimated stiffness is close to the actual stiffness of the experimental substructure. In the lower frequency system (a), the converged and experimental displacements are almost identical to the exact solution up to 2.5 Hz that is more than the double of the natural frequency. This excellent agreement indicates that the quadratic alpha method provides accurate simulation results for a wide frequency range for lower frequency systems. However, in the median frequency system (b), the converged and experimental displacements show agreement with the exact solution only up to 10 Hz, which is the natural frequency of the system. This agreement range means that the quadratic alpha method is accurate for the lower excitation input but not so for high excitation input beyond the natural frequency for median frequency systems. And, in the high frequency system (c), the frequency range for the agreement between the converged and experimental displacements and the exact solution is only up to 10 HZ, which is less than the half of the natural frequency. This limited agreement implies that for high frequency systems the quadratic alpha method can be used for quasi-static inputs, but it certainly not suitable for dynamic inputs. The above observation and discussion reveal that the application frequency range of the quadratic alpha method is highly dependent on the natural frequency of the system. And thus, relations between the system of interest and applicable simulation phenomenon (e.g., dynamic, quasi-static, and static loading) have to be carefully selected in the force based hybrid simulation using the quadratic alpha method.

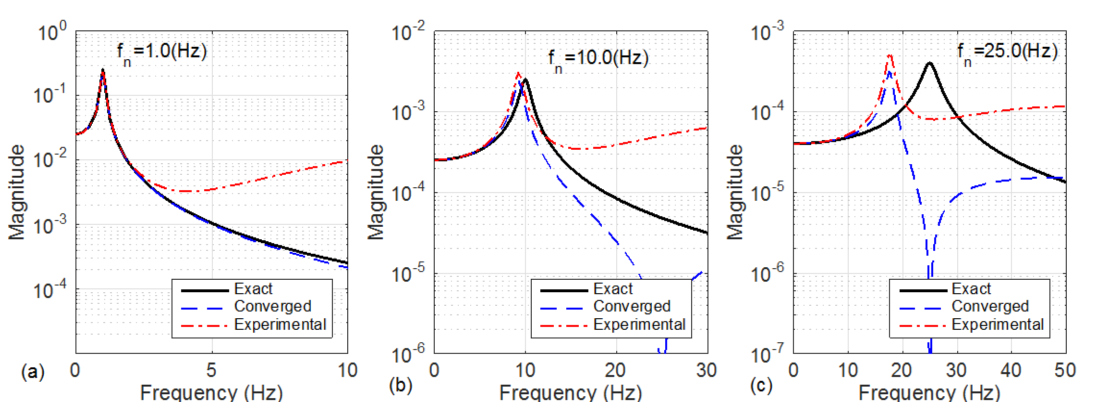

Fig.2 – Frequency responses of a single-degree-of-freedom system with the quadratic alpha method: (a) fn=1 (Hz), (b) fn=10 (Hz), and (c) fn=25 (Hz).

3.3 Effects of the stiffness estimation on stability

While the quadratic alpha method is proven to be stable at $\mu = 1$, the estimated stiffness in the algorithm cannot be always guaranteed equal to the true stiffness of the experimental system due to uncertainties and nonlinearities. The effects of the error in the estimated stiffness are investigated here. Fig.3 shows roots of the characteristic equations, the denominator of the transfer functions, and the stability assessment for different μ. The other parameters are the same in the previous section.

Because the characteristic equation is the fourth-order polynomial, there are four roots in each case. Two of the four roots are a pair of complex conjugate that stems from the eigenvalues of the dynamic model. These roots are located in the right hand side of the real-imaginary plot in (a) and are not sensitive to the stiffness ratio μ. For all of the cases, they are always within the unit circle. On the other hand, the remaining two roots that are attributed to the algorithm are sensitive to the change in μ; for $\mu < 1$, they are a pair of complex conjugate, but for $\mu \geq 1$, they are real numbers. And, when the stiffness ratio μ is greater than 1.4, one of the roots moves outside the unit circle. The stability of the quadratic alpha method judged from the locations of roots is plotted in Fig.3 (b). It can be seen that the algorithm becomes unstable if the stiffness ratio is greater than 1.4 while it is stable otherwise. This assessment tells us that the estimated stiffness in the quadratic alpha algorithm can be either underestimated or overestimated. But, if overestimated, it has to be less than 1.4 times the true stiffness.

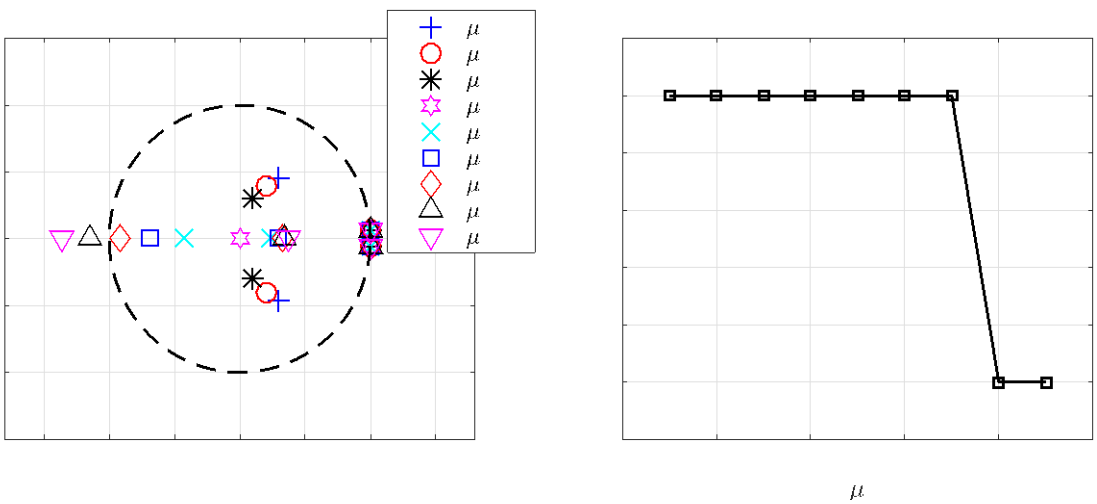

Fig.3 – Stability assessment: (a) roots of the characteristic equation and (b) the stability criteria.

4. Numerical simulation and validation

To investigate stability, accuracy, and characteristics of the quadratic alpha method, preliminary numerical simulations are carried out. This section presents the preliminary numerical simulation.

4.1 Structural simulation models and parameter settings

A single-degree-of-freedom system shown in Fig.4 is considered. The mass and damping coefficient of the model are $m = 2000$ (kg), $c = 1256.6$ (N$\cdot$sec/m), respectively. Three types of the restoring force are considered herein: (I) linear elastic; (II) linear hysteretic with friction; and (III) bilinear hysteretic. Parameters for the restoring forces are shown in Fig.4 (b). The other simulation parameters are following: $\alpha = 0.5$, $\beta = 0.3$, $\gamma = 0.6$, $\Delta t = 0.01$.

4.2 Structural simulation with earthquake, wind and coastal surge

The first simulation presented in this section is an earthquake loading. Fig.5 shows results from the earthquake simulation for the aforementioned three restoring force models. The input acceleration in this simulation is the 1995 Kobe earthquake KJM record with the peak acceleration scaled at 0.3g shown in Fig.5 (a). For a comparative purpose, the displacement time history from the nonlinear dynamic analysis is plotted in the figure. In this paper, the nonlinear dynamic analysis serves as a reference for the validation of the quadratic alpha method.

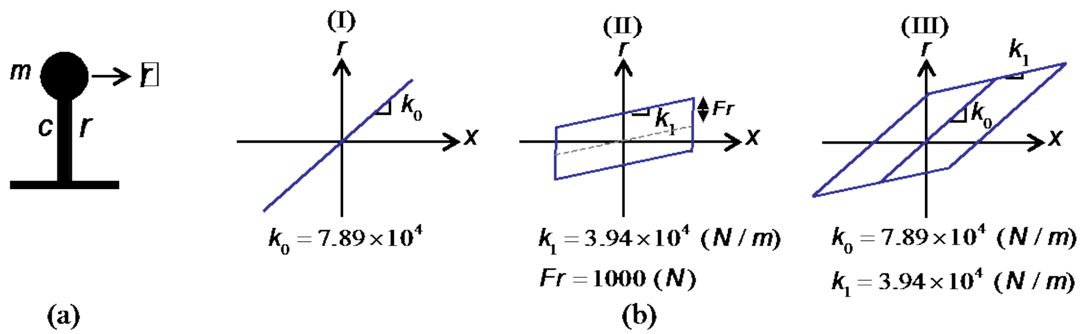

Fig.4 – Structural models for the preliminary numerical simulation: (a) an SDOF model; and (b) restoring force models.

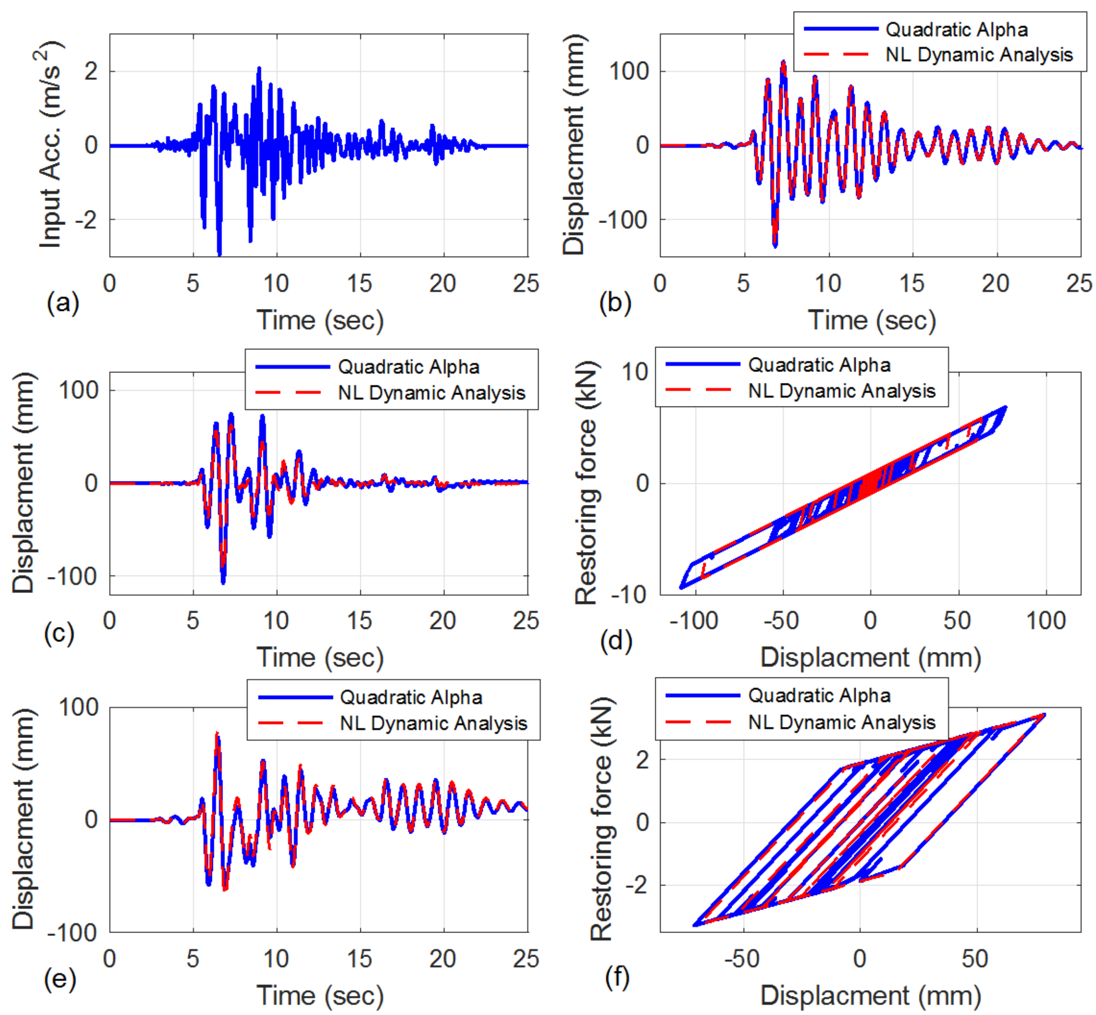

Fig.5 – Earthquake simulation: (a) input ground acceleration, the 1995 Kobe earthquake KJM record; (b)(c) and (d), displacement time histories for a linear elastic, linear with friction, and bilinear hysteretic model, respectively; (e) and (f) and hysteresis for the linear with friction and bilinear hysteretic model, respectively.

It is clear from Fig.5 (b) shows that the quadratic alpha method is stable and provides almost identical results with the reference nonlinear dynamic analysis in the linear elastic model (I). This level of accuracy is consistent with and expected from the investigation in the previous section. On the other hand, for the nonlinear models (II) and (III), the quadratic alpha method does not provide the same level of agreement with the nonlinear dynamic analysis (see Fig.5 (c-f)). While good agreement is seen in both the time history and hysteresis of the bilinear model, the displacement of the friction model has discrepancy with the reference. This difference is considered due to the limitation of the constant estimated stiffness in the quadratic alpha method; the estimated stiffness does not capture sudden change in stiffness seen in the friction model. Although it is not addressed in this study, the accuracy can be improved by incorporating an online tangent stiffness that is updated during the simulation. Overall, the earthquake simulation proves that the quadratic alpha method is a stable and accurate numerical integration algorithm for dynamic simulation and is a promising enabling tool for force-based hybrid simulation.

The next simulation is a wind loading on the structure. Fig.6 shows the time histories and power spectral densities of the input wind force and structural displacement. In this simulation, wind velocity time history is generated based on the conventional Kaimal spectrum (1972) with an assumption that the mean wind velocity is 10 m/s at 10 m height. Then, the wind force time history is calculated from the following formula: $F_D = 0.5\rho C_D A V^2$ where F_D is the wind force, V is the wind velocity, ρ is the air density, C_D is the drag coefficient, and A is the story area facing the wind. The structural model here is a linear elastic.

It can be seen from Fig.6 that the wind loading is more or less random excitation but the most wind power is on the low frequency side. Judging based on this fact, the wind simulation falls into the feasible simulation cases for the quadratic alpha method discussed in Fig.2. As expected, the structural displacement time history from the quadratic alpha method agrees well with the reference simulation. Most importantly, the quadratic alpha method provides accurate frequency domain response for the wind loading (see Fig.6 (d)). The simulation here demonstrates that the quadratic alpha method is applicable to wind simulation and can serve as a possible algorithm for force-based hybrid simulation for wind load.

Fig.6 – Application of the quadratic alpha method to wind simulation: (a) wind force time history; (b) structural displacement time history; (c) power spectram of the input wind force; and (d) power specturam of the structural displacement.

Applicability of the quadratic alpha method to coastal storm surge is also assessed in this paper. A time history of hydrodynamic force used for the structural simulation is generated from computational fluid dynamics (CFD) using the Volume-to-Fluid method. The configuration of the CFD is shown in Fig.7. At the time equal to zero, the gate is opened and the water surge propagates to the structure that is 1.3 m away from the gate. A velocity profile of a given time is shown in Fig.7 (b). The hydrodynamic force is calculated from the surface pressure on the front face of the vertical wall.

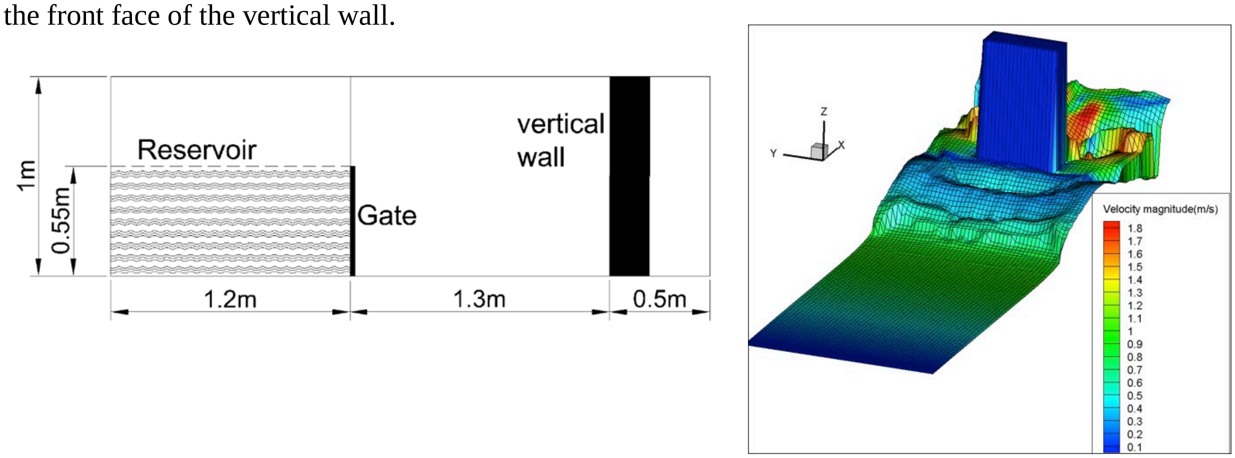

Fig.7– Computational fluid dynamic simulation to generate coastal storm surge load for the structures: (a) simulation configuration and (b) a velocity profile at a given time.

Fig.8 shows the time history of a scaled hydrodynamic force and structural simulation results from the quadratic alpha method. The bilinear hysteretic model is considered herein. It can be seen from Fig.8 (a) that the storm surge load first hits the structure at time equal to 0.5 second and has two distinct impulse-type peaks at 1.5 and 4 second. The critical dynamic phenomenon occurs within about 6 second. While some discrepancies are present, the displacement and force time histories as well as the hysteresis show very good agreement with those from the reference nonlinear dynamic analysis. The residual displacement after the surge is also very similar in both methods. While further investigation and validation are needed, this simulation exhibits feasibility of the quadratic alpha method for the coastal storm surge load.

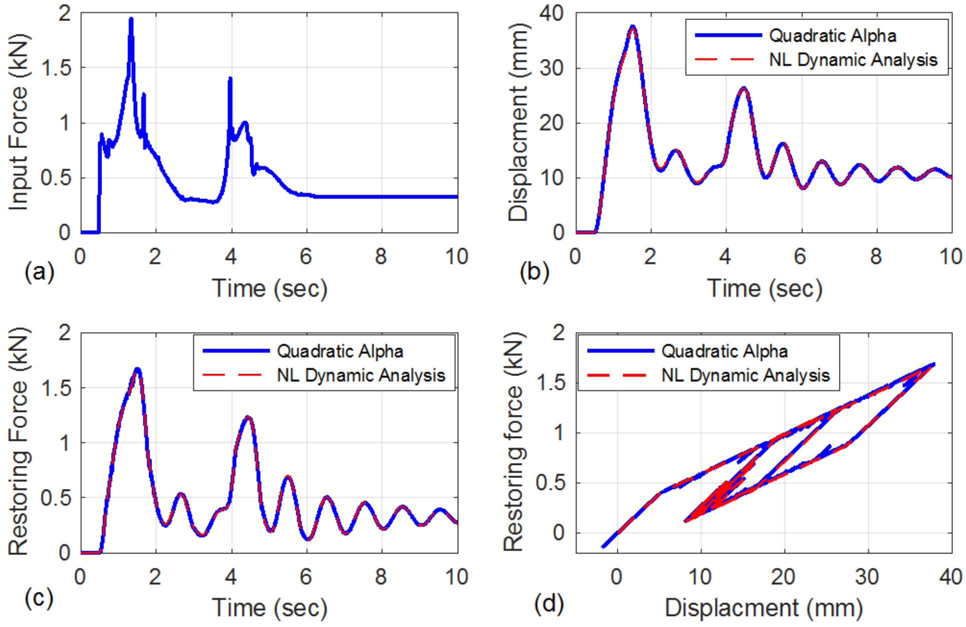

Fig.8 – Application of the quadratic alpha method to coastal storm surge: (a) strom surge load time history; (b) structural displacement time history; (c) restoring force time history; and (d) hysteresis.

5. Conclusion

This paper presented a new force-based explicit numerical integration algorithm, so-called quadratic-alpha method. The proposed method is based on the quadratic interpolation of the equation of motion and consists of pre-experimental, experimental, and post-experimental processes to enable hybrid simulation. The main difference between the proposed and existing numerical methods is that the quadratic alpha method provides the reference force that is to be imposed in the experiment instead of the reference displacement. Thus, the proposed method allows and serves as a framework for complete and sound force-based hybrid simulation.

Formulation and background theories of the quadratic alpha method as well as the implementation flowchart were presented first in the paper. Then, dynamic characteristics and stability of the method were discussed using discrete transfer functions. The stability assessment showed that the quadratic alpha method provide stable simulation for systems with different natural frequencies. And, if the estimated stiffness is less than 1.4 times the actual stiffness, the method is stable and reasonably accurate.

The numerical simulation of the quadratic alpha method was performed for earthquake, wind and coastal storm surge loads with three restoring force models. While some discrepancies were found between the quadratic alpha method and the reference nonlinear dynamic analysis for highly nonlinear hysteresis models, the method was proven to be stable and provide reasonable accuracy for all of the considered scenarios. The next critical steps are the experimental implementation and validation that are currently underway at Clarkson University.

6. Acknowledgements

The presented research is funded by the National Science Foundation under an award entitled 'CAREER: Advanced Acceleration Control Methods and Substructure Techniques for Shaking Table Tests (grand number CMMI-1503579)'.

7. References

[1] Nakata N, Dyke S, Zhang J, Mosqueda G; Shao X; Mahmoud H; Head M; Bletzinger M; Marshall G; Ou G; Song C (2014): Hybrid Simulation Primer and Dictionary, https://nees.org/resources/7702.

[2] Mahin S, Shing P. (1985): Pseudodynamic Method for Seismic Testing. *Journal of Structural Engineering*, **111**(7), 1482-1503.

[3] Nakashima M, Masaoka N (1999): Real-time on-line test for MDOF systems. *Earthuake Engineering and Structural Dynamics*, **28**(4), 393-420.

[4] Dimig J, Shield C, French C, Bailey F, Clark A (1999): Effective force testing: a method of seismic simulation for structural testing. *Journal of Structural Engineering*, **125**(9):1028–1037.

[5] Nakata N (2013): Effective force testing using a robust loop shaping controller. *Earthquake Engineering and Structural Dynamics*, **42**(2), 261–275.

[6] Kaimal J, Wyngaard J, Izumi Y, Coté O (1972): Spectral characteristics of surface-layer turbulence. *Quarterly Journal of the Royal Meteorological Society*, **98** (417), 563-589.